Chemical Shifts in Proteins: An *Ab Initio* Study of Carbon-13 Nuclear Magnetic Resonance Chemical Shielding in Glycine, Alanine, and Valine Residues†

Angel C. de Dios, John G. Pearson,‡ and Eric Oldfield*

Contribution from the Department of Chemistry, University of Illinois at Urbana-Champaign, 505 South Mathews Avenue, Urbana, Illinois 61801

Received June 1, 1993®

Abstract: Using gauge-including atomic orbital self-consistent field *ab initio* quantum chemical methods, we have computed the effects of bond lengths, bond angles, and torsion angles on the carbon-13 chemical shielding of C^{α} (and C^{β}) sites in model fragments for glycine, alanine, and valine residues in proteins. Predicted chemical shieldings are highly sensitive to bond length variations, and we show that it is essential to relax or energy minimize protein structures (to remove large errors associated with bond length uncertainties) in order to successfully predict experimental ^{13}C NMR spectra.

1. Introduction

Recently, the prediction of folding-induced ^{1}H, ^{13}C, ^{15}N, and ^{19}F chemical shifts in proteins using *ab initio* methods has been shown to be feasible.[1] In particular, it has been demonstrated that, by separating the secondary chemical shift into short-range (electronic) and long-range (magnetic and electrostatic) contributions,[2] the problem of carrying out *ab initio* chemical shielding calculations on proteins becomes much more tractable than might at first be thought. Severe limitations of disk space and computational time are avoided by assigning basis functions only to those atoms in close proximity to the nucleus in question, with the rest of the protein being represented by a point charge field. As a result of using this approach, new insights into the origins of folding-induced shifts have become available. For example, the ^{19}F chemical shift nonequivalencies observed in [5-F]Trp-labeled *Escherichia coli* galactose binding protein have been found to be due primarily to long-range electrostatic field effects.[1] On the other hand, the ^{13}C chemical shifts of the α- and β-carbon nuclei in the Ala residues of staphylococcal nuclease are dominated by the torsional angles ϕ and ψ.[1] For the ^{15}N sites in Val residues, there appears to be a combination of short- and long-range contributions, including strong hydrogen bonding, although torsion angles once again dominate. The intrinsic relationships between chemical shifts and secondary structure open new avenues for refining and predicting protein structure, and because of the dominance of short-range effects on their shielding, C^{α} and C^{β} sites in proteins appear to be excellent candidates for initial explorations of these topics.

The degree of success attained in reproducing the chemical shifts in any system is strongly dependent upon the quality of the structure used in a self-consistent field (SCF) calculation, since the calculated chemical shift (or shielding) is extremely sensitive to the local structure. The protein staphylococcal nuclease, which was employed in the previous study,[1] has a relatively well-resolved X-ray structure (1.65 Å),[3] but even at this high resolution, the structure still needed to be relaxed or energy minimized in order to obtain good agreement with experiment.[1] For example, bond lengths need to be highly accurate (within 0.005 Å), as implied by earlier studies on small molecules.[4-8] Unfortunately, X-ray (and NMR) structures available for proteins do not yet satisfy this requirement. Consequently, direct use of X-ray (or solution NMR) structures will not generally yield theoretical chemical shifts strongly correlated with the experimentally observed values. In this work, we show that the chemical shieldings for C^{α} and C^{β} are strongly influenced by the following local structural parameters: bond lengths, bond angles, and dihedral angles. Evaluating which of these parameters dominate the experimental chemical shifts is essential before one can elucidate (or refine) protein structures from experimental chemical shifts, and since the number of observables is less than the number of variables which might be involved, the task becomes complex. Fortunately, as we show below, it is possible to derive from theory the dependence of shielding on each of these parameters, separately, thereby opening up the prospect of refining and/or predicting protein structure via use of chemical shift information.

We can evaluate the bond length and bond angle shielding derivatives—how the chemical shift changes with bond length or angle—as well as determine from shielding surfaces how the observed shifts (or computed shieldings) vary with, for example, ϕ and ψ. As we demonstrate in the text, our results show that protein structures can be relaxed to yield structures of more uniform bond length, thereby removing much of the chemical shift scatter due to the relatively low resolution (from an SCF standpoint) of existing structures. Moreover, if the torsion angles ϕ and ψ change during energy minimization (as they do), then use of shielding surfaces *and* the shielding derivatives permits the rapid prediction of an experimental spectrum without involving *ab initio* calculations for each site, although of course individual amino acid shielding surfaces still have to be calculated first.

† This work was supported by the United States National Institutes of Health (Grants HL-19481 and (in part) GM-40426), by the American Heart Association (Grant AHA 92-013340) with funds provided in part by the American Heart Association, Illinois Affiliate, Inc., and by the Graduate Research Board of the University of Illinois.

‡ United States Public Health Service Postdoctoral Fellow (Grant GM-14545).

® Abstract published in *Advance ACS Abstracts,* September 15, 1993.

(1) de Dios, A. C.; Pearson, J. G.; Oldfield, E. *Science* **1993**, *260*, 1491.
(2) de Dios, A. C.; Oldfield, E. *Chem. Phys. Lett.* **1993**, *205*, 108.
(3) Loll, P. J.; Lattman, E. E. *Proteins: Struct., Funct., Genet.* **1989**, *5*, 183.
(4) Fowler, P. W.; Riley, G.; Raynes, W. T. *Mol. Phys.* **1981**, *42*, 1463.
(5) Raynes, W. T.; Fowler, P. W.; Lazzeretti, P.; Zanasi, R.; Grayson, M. *Mol. Phys.* **1988**, *64*, 143.
(6) Jameson, C. J.; de Dios, A. C.; Jameson, A. K. *J. Chem. Phys.* **1991**, *95*, 1069.
(7) Jameson, C. J.; de Dios, A. C.; Jameson, A. K. *J. Chem. Phys.* **1991**, *95*, 9042.
(8) Jameson, C. J.; de Dios, A. C. *J. Chem. Phys.* **1993**, *98*, 2208.

0002-7863/93/1515-9768$04.00/0

Table I. Geometrical Parameters for the Fragments Used in *Ab Initio* Calculations

parameter	fragment		
	glycine	alanine	valine
C^{α}–C^{β} (r, Å)		1.538	1.550
C^{α}–C^{0} (r, Å)	1.540	1.548	1.550
C^{α}–N (r, Å)	1.470	1.471	1.480
C–H (r, Å)	1.090	1.090	1.090
N–C^{α}–C^{0} (θ, deg)	113.9	112.9	110.9
N–C^{α}–C^{β} (θ, deg)		109.0	110.1
C^{β}–C^{α}–C^{0} (θ, deg)		104.6	111.2

However, these should be applicable to *all* proteins, without modification. NMR chemical shielding calculations thus offer new ways of refining existing (X-ray and NMR) protein structures, as well as ways of predicting new ones, based on *ab initio* quantum chemical analyses of experimental chemical shifts.

2. Computational Aspects

Chemical shielding calculations were carried out by using the GIAO (gauge-including atomic orbitals) method[9] implemented in the TEXAS 90 program of Pulay, Wolinski, and Hinton.[10] The following fragments were investigated:

Glycine

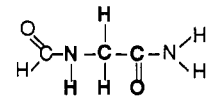

Alanine

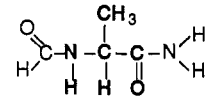

Valine

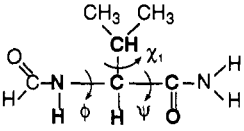

An attenuated or locally dense basis set scheme was employed[11] in which a 6-311++G(2d,2p) basis was provided for the bold 'core' atoms, above, while a 6-31G basis was used for the rest of the atoms in each fragment. Chemical shieldings were calculated for both C^{α} and C^{β} (where applicable) at various geometries. This was done by systematically varying one structural parameter while keeping the others constant. We designate the locus of shielding values obtained as a trace on the multidimensional shielding surface. We express these shielding traces in terms of Taylor series expansions at the geometries given in Table I:

$$\sigma(r) = \sigma(r_o) + \left(\frac{\partial\sigma}{\partial r}\right)_{r_o}(r - r_o) + \frac{1}{2}\left(\frac{\partial^2\sigma}{\partial r^2}\right)_{r_o}(r - r_o)^2 + \frac{1}{6}\left(\frac{\partial^3\sigma}{\partial r^3}\right)_{r_o}(r - r_o)^3 + \ldots \quad (1)$$

$$\sigma(\theta) = \sigma(\theta_o) + \left(\frac{\partial\sigma}{\partial\theta}\right)_{\theta_o}(\theta - \theta_o) + \frac{1}{2}\left(\frac{\partial^2\sigma}{\partial\theta^2}\right)_{\theta_o}(\theta - \theta_o)^2 + \frac{1}{6}\left(\frac{\partial^3\sigma}{\partial\theta^3}\right)_{\theta_o}(\theta - \theta_o)^3 + \ldots \quad (2)$$

where r is a generic bond length and θ is a generic bond angle. The geometries used are those obtained after extensive minimization (15 000 steps via the Discover Program, Biosym Technologies, Inc., San Diego, CA).

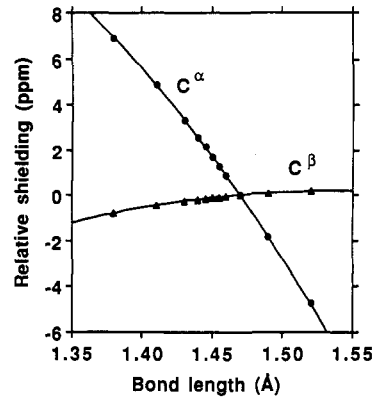

Figure 1. C^{α} and C^{β} relative shielding as a function of C^{α}–N bond length in an alanine fragment: ●, C^{α}; ▲, C^{β}.

For bond length studies, shieldings were calculated for bond lengths ranging within ±0.1 Å of the values given in Table I. Bond angles were varied by up to ±10°. These ranges are representative of the values found for Gly, Ala, and Val residues in protein X-ray structures. Also, the influence of the valine side chain torsional angle, χ_1, was examined, with χ_1 being incremented in 10° steps.

The wide range of ϕ and ψ values observed in proteins necessitates a determination of shielding values with simultaneous variation of both dihedral angles. This is discussed in detail elsewhere[12] and involves the construction of a shielding surface in 'Ramachandran space', quite analogous to the empirical shielding (or secondary chemical shift) surfaces presented by Spera and Bax.[13] A separate study indicated that the results obtained using the smaller (6-311G**) basis set[12] are essentially identical to the attenuated basis set results described above.

Calculations were carried out in our laboratory by using a cluster of RISC computers (International Business Machines, Corp., Austin, TX) equipped with a total of 0.3 GB of RAM and 26 GB of disc and having a peak theoretical speed of ~0.6 Gflops, as well as at the University of Illinois at Chicago on an IBM RISC 6000/Model 560 computer.

3. Results and Discussion

We show in Figure 1 typical shielding results for C^{α} and C^{β} sites in the alanine fragment shown above as a function of C^{α}–N bond length, and in Figure 2, we show relative C^{α} shieldings of the glycine, alanine, and valine fragments as a function of the N–C^{α}–C^{0} bond angle. These and related data sets were fitted to eqs 1 and 2, and the bond length shielding derivatives deduced are presented in Table II, while Table III gives the bond angle shielding derivatives. The negative sign of the first derivative, which is generally observed in studies involving small molecules,[4-8] is evident here also. However, the shielding of Ala C^{β} has a shape resembling that of the intermolecular shielding functions obtained for rare gas atoms,[14] when plotted against bond lengths not involving the β-carbon directly. These observations agree well with the predicted behavior of $\partial\sigma/\partial r$ over a wide range of internuclear separations in diatomic molecules,[8] where it has been shown that this derivative is negative at short internuclear separations and positive at larger distances.

The three fragments show very similar derivatives with respect to bond lengths, as shown in Table I. For all three residues, shielding is found to be most sensitive to the C^{α}–N bond length, with alanine and valine showing remarkably similar derivatives,

(9) Ditchfield, R. *J. Chem. Phys.* **1972**, *56*, 5688.
(10) Pulay, P.; Wolinski, K.; Hinton, J. F. *The TEXAS Program*; University of Arkansas: Fayetteville, AR, 1991.
(11) Chesnut, D. B.; Moore, K. D. *J. Comput. Chem.* **1989**, *10*, 648.
(12) Pearson, J. G.; de Dios, A. C.; Oldfield, E. Unpublished results.
(13) Spera, S.; Bax, A. *J. Am. Chem. Soc.* **1991**, *113*, 5490.
(14) Jameson, C. J.; de Dios, A. C. *J. Chem. Phys.* **1992**, *97*, 417.

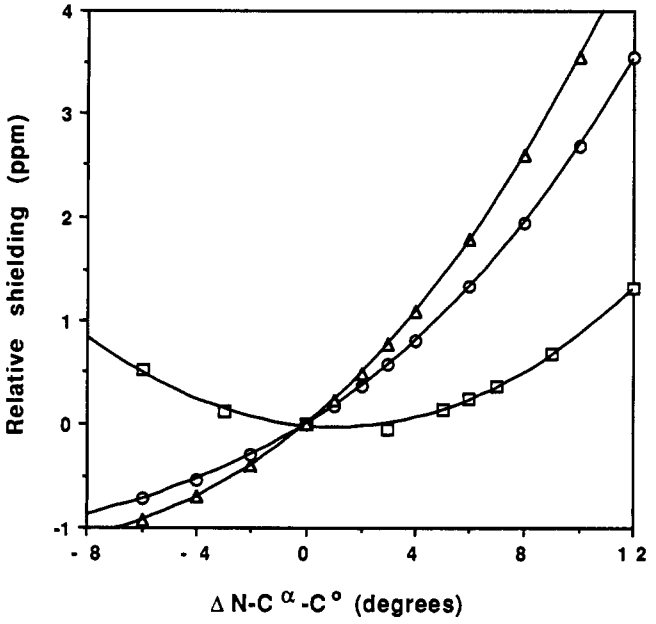

Figure 2. C^{α} relative shielding of glycine, alanine, and valine fragments as a function of the N–C^{α}–C^{0} angle; □, glycine; ○, alanine; △, valine. See the text for details.

Table II. Shielding Derivatives with Respect to Bond Length (ppm/Å^{n})[a]

fragment	bond type	derivative order (n)	C^{α}	C^{β}
glycine	C^{α}–C^{0}	1	−48.4	
		2	−102.7	
		3	138.4	
	C^{α}–N	1	−69.0	
		2	−243.0	
		3	240.0	
alanine	C^{α}–C^{β}	1	−15.6	−36.1
		2	−134.1	−171.0
		3	214.0	198.6
	C^{α}–C^{0}	1	−56.9	10.3
		2	−106.8	−75.5
		3	134.4	218.1
	C^{α}–N	1	−88.0	6.8
		2	−261.2	−81.7
		3	105.6	134.1
	C^{α}–H^{α}	1	−56.8	−7.4
		2	−132.1	−8.5
		3	159.4	14.0
valine	C^{α}–C^{β}	1	−17.3	−68.9
		2	−96.6	−185.9
		3	204.0	199.8
	C^{α}–C^{0}	1	−60.3	3.4
		2	−111.9	−54.5
		3	158.4	112.8
	C^{α}–N	1	−84.1	9.5
		2	−266.0	−58.6
		3	177.1	45.6

[a] The derivatives represent the values $(\partial\sigma/\partial r)$, $(\partial^2\sigma/\partial r^2)$, and $(\partial^3\sigma/\partial r^3)$ (see text, eq 1) and are given in units of ppm/Å, ppm/Å^2, and ppm/Å^3.

especially for C^{α}–N and C^{α}–C^{0}. There are larger differences for the C^{α}–C^{β} derivative, due presumably to the fact that alanine and valine differ in their side chains. The fact that the alanine and valine backbone bond length shielding derivatives are so similar appears to be consistent with the observation that the corresponding C^{α}–N and C^{α}–C^{0} derivatives for glycine are also quite similar to those of Ala and Val, even though there is no α-alkyl substituent in Gly. This clearly indicates that short-range effects on shielding are highly localized, which will hopefully extend the applicability of these shielding traces to other amino acids as well.

Table III. Shielding Derivatives with Respect to Bond Angle (ppm/deg^{n})[a]

fragment	bond angle type	derivative order (n)	C^{α}	C^{β}
glycine	N–C^{α}–C^{0}	1	0.11	
		2	0.022	
		3	0.000 22	
alanine	N–C^{α}–C^{β}	1	−0.10	0.29
		2	0.014 6	−0.018
		3	0.000 004	0.000 038
	N–C^{α}–C^{0}	1	0.20	0.001 4
		2	0.019	−0.005 0
		3	0.001 2	−0.000 22
	C^{β}–C^{α}–C^{0}	1	0.20	0.038
		2	0.024	−0.024
		3	0.001 6	−0.000 20
valine	N–C^{α}–C^{β}	1	−0.10	0.34
		2	0.015	−0.024
		3	−0.000 050	0.000 001
	N–C^{α}–C^{0}	1	0.27	0.14
		2	0.025	−0.003 0
		3	0.000 78	−0.000 18
	C^{β}–C^{α}–C^{0}	1	0.41	−0.75
		2	0.17	−0.22
		3	0.019	−0.034

[a] The derivatives represent the values $(\partial\sigma/\partial\theta)$, $(\partial^2\sigma/\partial\theta^2)$, and $(\partial^3\sigma/\partial\theta^3)$ (see text, eq 2) and are given in units of ppm/deg, ppm/deg^2, and ppm/deg^3.

The dependence of shielding on bond angle is more complex than its dependence on bond length. Within the range of values of these parameters found in X-ray structure of proteins, shielding as a function of bond length can be approximated by a linear function, while shielding traces with respect to bond angles show significant curvature, as shown in Figure 2. The shielding dependence for C^{α} on the N–C^{α}–C^{0} bond angle for the Gly, Ala, and Val fragments is shown in Figure 2. Only relative shieldings are shown, in order to facilitate comparisons between the different residues. A shielding value of 0.0 ppm was assigned to the conformation that has the minimum SCF energy (Ala = 113°, Gly = 108°, and Val = 109°). Angles are also referenced to this low-energy conformation. Once again, the similarity between alanine and valine is striking. Glycine, on the other hand, shows a minimum close to the tetrahedral angle, indicating that shielding is not very sensitive to bond angle. However, the shielding function becomes somewhat steeper at larger bond angles, as shown in Figure 2. Bond angle shielding derivatives for each of the three residues are given in Table III.

The bond length and bond angle shielding derivatives shown in Tables II and III are of use in predicting experimental ^{13}C NMR spectra, since they permit shielding corrections caused by scatter in the experimental parameter. However, additional information on the ϕ and ψ dependence of the shieldings is also required in order to make complete shielding (chemical shift) predictions. This topic is discussed in detail elsewhere,[12] but in order to demonstrate use of the complete shielding derivative/shielding surface approach, we show in Figure 3 computed C^{α} and C^{β} shieldings for an Ala fragment as a function of ϕ and ψ. These $\sigma(\phi,\psi)$ surfaces can be used to estimate experimental shifts (or shieldings) for a given ϕ and ψ, then the bond length and bond angle derivatives can be used to make shielding corrections, due to bond length/bond angle distortions. Note that the two surfaces are only weakly anticorrelated. This is an important point, since, in the future, the fact that C^{α} and C^{β} shifts are only weakly related should make it possible to use *both* pieces of chemical shift information to deduce structure.

Now, in order to examine the applicability of the various shielding derivatives in predicting shielding values, it is necessary to check their independence, or additivity. Otherwise, it would be necessary to calculate complete multidimensional surfaces, instead of just traces. For bond length derivatives, we thus carried out a set of calculations in which two bond lengths, C^{α}–N and

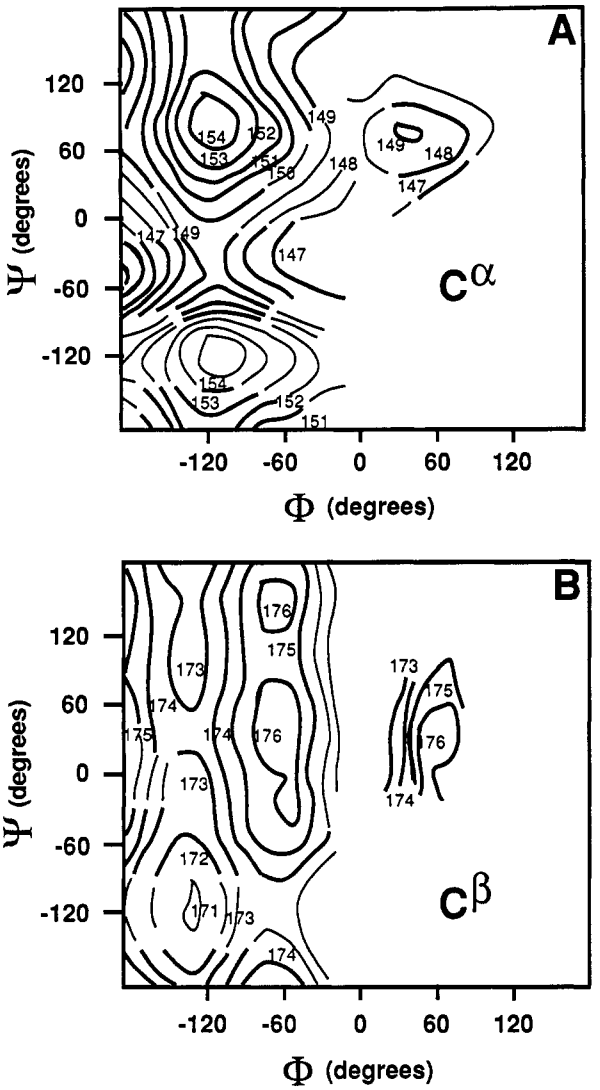

Figure 3. C^{α} and C^{β} shielding surfaces for alanine fragments: **A**, C^{α}; **B**, C^{β}. Dark contours are drawn over regions where points were actually calculated. Based on results derived in ref 12.

C^{α}–C^{0}, were altered simultaneously. The results of these calculations are shown in Figure 4, which clearly demonstrates that the individual bond length effects can be treated as additive, and hence can be evaluated separately. This observation is consistent with the additivity previously observed for secondary isotope shifts.[15]

We also investigated the separability of bond length and torsional effects, by computing for C^{α} of the Ala fragment the first-, second-, and third-order derivatives of the C^{α}–C^{β}, C^{α}–C^{0}, and C^{α}–N bond length shielding functions. Figure 5 shows the relative C^{α} shielding as a function of the C^{α}–N bond length for three (ϕ,ψ) pairs: $\phi = -57.7$, $\psi = -50.5$ (helix); $\phi = 55.0$, $\psi = 50.0$ (turn); $\phi = -71.4$, $\psi = 140.0$ (sheet). Clearly, the C^{α}–N shielding derivatives are independent of ϕ and ψ, and the three sets of bond length shielding derivatives as a function of ϕ and ψ are tabulated in Table IV. Thus, it seems likely that we can make bond length corrections at any ϕ and ψ values.

Armed with these shielding traces, it should now be possible to predict chemical shifts given a set of structural parameters without having to perform full *ab initio* calculations for each site of interest. Similarly, knowledge of the shielding derivatives enables an estimate of the various contributions to shielding for a given protein structure. For example, we show in Figure 6 the

(15) Jameson, C. J.; Osten, J. J. *Annu. Rep. NMR Spectrosc.* **1986**, *17*, 1.

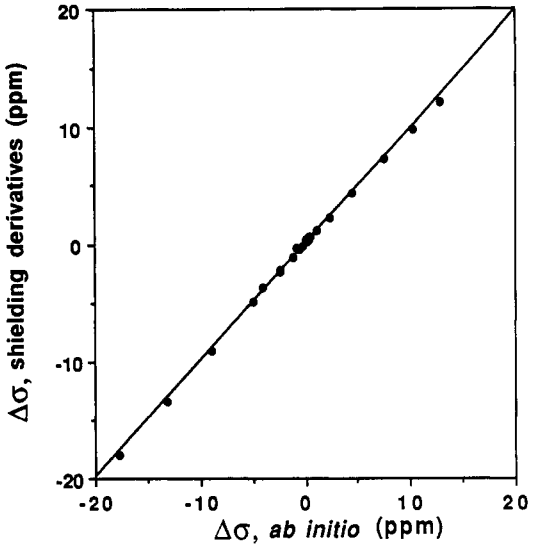

Figure 4. Additivity of structural effects on Ala C^{α} relative shielding. The graph shows the results of varying the C^{α}–N and C^{α}–C^{0} bond lengths simultaneously using either a full *ab initio* treatment (horizontal axis) or by using the bond length shielding derivatives (vertical axis).

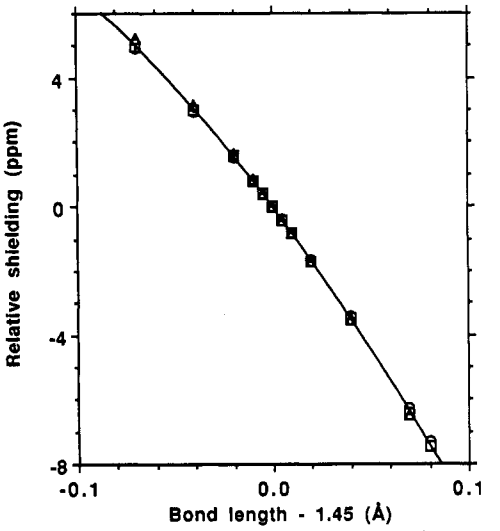

Figure 5. Alanine C^{α} relative shielding traces with respect to C^{α}–N bond length, evaluated at various ϕ and ψ values: ○, $\phi = -57.7°$, $\psi = -50.5°$ (helix); □, $\phi = 55.0°$, $\psi = 50.0°$ (turn); △, $\phi = -71.4°$, $\psi = 140.0°$ (sheet). The relative shielding at $r = 1.45$ Å is taken to be 0.0 ppm.

Table IV. Shielding Derivatives for C^{α} in an Alanine Fragment with Respect to Bond Length (ppm/Å) Evaluated at Different Torsion Angles

		torsion angles (ϕ and ψ, deg)		
bond type	derivative order (n)	$\phi = -71.4$, $\psi = 140.0$ (sheet)	$\phi = -57.7$, $\psi = -50.5$ (helix)	$\phi = 55.0$, $\psi = 50.0$ (turn)
C^{α}–C^{β}	1	−15.6	−9.90	−22.9
	2	−134.1	−133.0	−127.7
	3	214.0	239.1	269.4
C^{α}–C^{0}	1	−56.9	−62.7	−57.4
	2	−106.8	−97.8	−100.1
	3	134.4	169.4	127.2
C^{α}–N	1	−88.0	−85.9	−87.8
	2	−261.2	−278.1	−299.1
	3	105.6	79.8	116.3

range of C^{α} chemical shift values that were obtained for the alanine residues in the staphylococcal nuclease X-ray structure determined by Loll and Lattmann,[3] due to scatter in C^{α}–N bond length. Figure 6 (top) shows the range in shielding due to C^{α}–N bond length variation in the original X-ray coordinates, while Figure

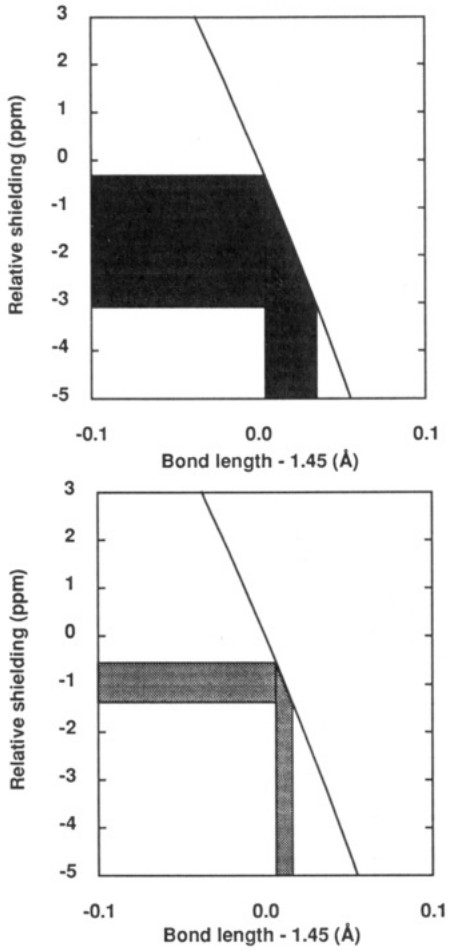

Figure 6. Range of shielding nonequivalence (shaded region) due to a spread in C^{α}–N bond length values found in staphylococcal nuclease: **A**, unminimized X-ray structure (ref 3); **B**, with 2000 steps of steepest descents minimization, ligand-free, solvated structure (see text for details).

6 (bottom) is derived from a 2000-step steepest descents minimization of a solvated, unligated structure. For SNase, we find that both ligated and unligated unminimized structures give poor accord with ligated and unligated solution NMR results.[16] Upon minimization, both X-ray structures yield improved correlation with experiment, although the best agreement is obtained when comparing ligand-free solution NMR chemical shifts with those predicted from a ligated structure, but energy minimized in the absence of Ca^{2+}/pdTp.[16] While this procedure appears unorthodox, our results for C^{α} of glycine and valine in SNase also show the best agreement with the solution NMR results when using the ligand-free "ligated" structure,[16] which suggests to us either that the overall ligand-free solution conformation may be closer to that of the ligated crystal structure, or simply that the ligated X-ray structure is more refined. In any case, for calmodulin, things are much simpler, and we find very significant improvements in C^{α} shielding predictions for each of Gly, Ala, and Val, on energy minimization.[16] Moreover, there are significant improvements in chemical shift predictions when using a more recent, highly refined calmodulin X-ray structure.[16] Thus, relaxation substantially eliminates the large bond length variations existing in unminimized X-ray structures and gives in most cases much better accord with experimental chemical shift observations, but a very good initial structure is still a prerequisite.

For many residues, it will be necessary to compute additional surfaces in order to take into account, e.g., side chain (χ_1, χ_2) or backbone (ω) torsional effects. While these add to the complexity

(16) Laws, D.; de Dios, A. C.; Oldfield, E. *J. Biomol. NMR*, in press.

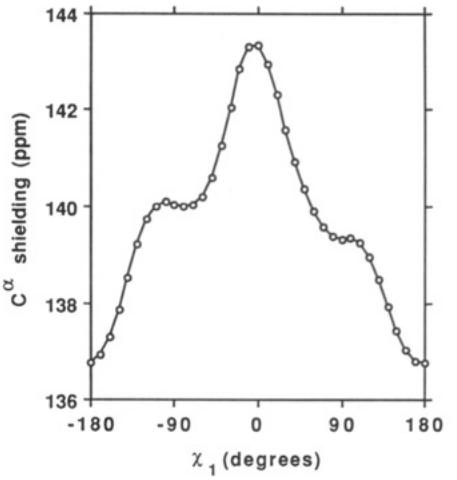

Figure 7. $^{13}C^{\alpha}$ shielding for a valine fragment ($\phi = -138.6°, \psi = 139.7°$), as a function of χ_1.

of the task of producing generally useful shielding surfaces, with the additional shielding surfaces come additional pieces of chemical shift information. For example, for valine, we have

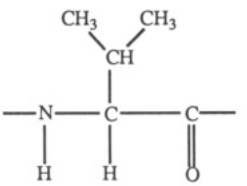

in which we have C^{α}, C^{β}, $C^{\gamma 1}$, $C^{\gamma 2}$, C^{0}, and N^{H}—a total of six heavy atom shifts, plus H^{α}, H^{N}, H^{β}, $H^{\gamma 1}$, and $H^{\gamma 2}$—five proton shieldings, many of which should provide valuable structural information. Conversely, there are 11 pieces of chemical shift information which need to be explained by a given protein structure, or set of structures (or possibly even a trajectory).

By way of example, let us consider the effects of χ_1 on shielding. For alanine, shielding of the β-carbon is not very sensitive to the side chain torsion angle, χ_1. The difference in shielding of the β-carbon between a staggered and an eclipsed conformation is only 0.3 ppm, with the staggered form more shielded. On the other hand, the shielding of the α-carbon is 3.5 ppm less shielded in the staggered than in the eclipsed conformation, although of course for alanine only a rotationally averaged value will be seen in solution. For larger residues, lack of symmetry leads to different shielding values for the different possible side chain conformations, and in Figure 7, we show how the C^{α} shielding in Val is affected by χ_1 in a typical sheet fragment ($\phi = -138.6$, $\psi = 139.7$). The three staggered conformations give the following shielding values: 136.8 ppm ($\chi_1 = 180°$), 140.2 ppm ($\chi_1 = -60°$), and 139.9 ppm ($\chi_1 = 60°$). In the case of valine residues in staphylococcal nuclease, only $\chi_1 = 180°$ and $-60°$ are found.[13] From the χ_1 shielding trace, this results in a 3.4-ppm contribution to the chemical shift range for the α-carbons of valine residues, which is a substantial fraction of the total experimentally observed chemical shift range of 6.0 ppm.[17] In qualitative agreement with this prediction, it is found experimentally that the valine residues with $\chi_1 = 180°$, on the average, are 2.3 ppm more shielded that those with $\chi_1 = 60°$, in staphylococcal nuclease. In future work, it should be possible to compute C^{α}, C^{β}, and C^{γ} shifts for valine, as a function of the three χ_1 torsions, and probe backbone and side chain structures via use of multiple shielding restraints.

We now briefly consider how one might be able to use some of the ideas we have presented above. Table V presents the geometric parameters of alanine residues derived from the X-ray

(17) Wang, J.; Hinck, A. P.; Loh, S. N.; Le Master, D. M.; Markley, J. L. *Biochemistry* **1992**, *31*, 921.

Table V. Mean and Standard Deviations of the Geometrical Parameters of Alanine Residues Found in Staphylococcal Nuclease[3] and a Vertebrate Calmodulin[18]

	staphylococcal nuclease		calmodulin	
parameter	X-ray	minimized[a]	X-ray	minimized[b]
C^{α}–C^{β} (Å)	1.527(0.012)	1.536(0.004)	1.527(0.006)	1.535(0.002)
C^{α}–C^{0} (Å)	1.525(0.009)	1.550(0.004)	1.521(0.010)	1.551(0.004)
C^{α}–N (Å)	1.474(0.014)	1.472(0.003)	1.467(0.006)	1.470(0.002)
N–C^{α}–C^{0} (deg)	109.3(2.9)	113.4(1.4)	112.1(2.7)	113.7(0.9)
N–C^{α}–C^{β} (deg)	110.3(2.9)	108.5(0.5)	109.7(1.5)	109.0(0.8)
C^{β}–C^{α}–C^{0} (deg)	110.6(1.6)	111.4(0.7)	111.7(1.5)	112.2(0.7)

[a] Energy minimized value, 14 000 steps of steepest descents. [b] Energy-minimized value, 10 000 steps of steepest descents.

structures of staphylococcal nuclease[3] and a vertebrate calmodulin,[18] together with their energy-minimized counterparts. By combining this information with the theoretical shielding traces presented in this work, it is possible to predict the various contributions to the shielding nonequivalencies, and their improvement on relaxation. The effects of the bond lengths, for example, are quite obvious, as shown in Figure 6. The variations in bond lengths of the same type of residue in a single-protein X-ray structure lead to chemical shift nonequivalencies that are almost as large as the experimental chemical shift range. For this reason, direct use of the coordinates from a given unrelaxed X-ray structure to calculate shielding will not generally give a good correlation with experiment. This is not to say that, e.g., the alanine residues in a protein all have identical bond lengths, only that the spread of values currently found in unrelaxed X-ray structures cannot be reconciled with the observed chemical shift (shielding) patterns. On the basis of the results presented here, it thus appears that ϕ and ψ are the primary determinants of C^{α} shielding, with bond lengths primarily contributing to correctable "error terms".

Evaluation of exact bond lengths and angles is a difficult problem and cannot simply be deduced from the shielding traces. However, there is still hope for evaluating absolute bond lengths from chemical shifts, for example, via analysis of complete shielding tensors, as well as by considering the *absolute* shielding values, instead of just comparing relative shifts (or shieldings). Using the absolute shielding value given by Jameson et al.[19] for a cylindrical sample of liquid tetramethylsilane at 300 K (186.4 ppm), the calculated shieldings in our previous work[1] are uniformly displaced by about 12 ppm from the experimental values, the experimental values being lower. Since these calculations were only performed at the SCF level, and electron correlation effects have been found to make ^{13}C even more shielded in small molecules (by about 5 ppm for CH_4[20]), the absolute shieldings are displaced in a direction that is consistent with the idea that the bond lengths found in protein X-ray structure may be somewhat shorter than the rovibrationally averaged values found in solution. The zero-point rovibrational correction for $^{13}CH_4$ in an isolated molecule calculated by Raynes et al.[5] is –3.9 ppm. These types of corrections could be even larger for α-carbons in amino acid residues in proteins, in which the carbon atoms will be involved in many low-frequency vibrational modes. Thus, the constant offset of 12 ppm may be accounted for, in part, by rovibrational corrections.

4. Conclusions

The results we have described above are important since they represent the first detailed study of the effects of bond lengths, bond angles, and torsion angles on ^{13}C NMR chemical shifts of amino acid residues (or fragments) in proteins. ^{13}C NMR chemical shifts appear to be useful for investigating protein structure, and in the future, it can be expected that ^{1}H, ^{13}C, and ^{15}N chemical shifts will all play an important role in protein structural analyses. The use of shielding surfaces appears to be quite promising, since ϕ and ψ information, independent of NOE or J-coupling results, can be obtained.

Acknowledgment. We thank Professors P. Pulay and J. F. Hinton and Dr. K. Wolinski, for providing us with a copy of their TEXAS 90 program, and Professors C. J. Jameson and A. K. Jameson, for helpful discussions and use of their IBM 6000/560 computer.

(18) Chattopadhyaya, R.; Meador, W. E.; Means, A. R.; Quiocho, F. *J. Mol. Biol.* **1992**, *228*, 1177.

(19) Jameson, A. K.; Jameson, C. J. *Chem. Phys. Lett.* **1987**, *134*, 461.

(20) Kutzelnigg, W.; van Wüllen, Ch.; Fleischer, U.; Franke, R.; Mourik, T. v. In *Nuclear Magnetic Shieldings and Molecular Structure*; Tossell, J. A., Ed.; Kluwer Academic Publishers: Dordrecht, The Netherlands, 1993.